

Low-temperature expansion of a spatially frustrated isotropic lattice model

A. Berera

Department of Physics, University of California, Berkeley, California 94720

K. A. Dawson

Department of Chemistry, University of California, Berkeley, California 94720

(Received 15 May 1989)

A low-temperature expansion of an isotropic, spatially frustrated lattice model with nearest-neighbor, second-, and third-nearest-neighbor interactions is presented. The zero-temperature states of this model are known exactly. For some regions of parameter space there is an infinity of zero-temperature states, although the ground-state entropy per spin is zero at zero temperature. In general one expects fluctuations at finite temperature to break the degeneracy on the zero-temperature-state manifold. When the zero-temperature states are regular or periodic, it is possible to characterize them and to apply the low-temperature expansion to break this degeneracy in a rigorous way. In the present paper we carry out such a calculation. However, we also have examined regions of parameter space where the degenerate states are irregular. A method is proposed that permits one to resolve between degenerate irregular states. It consists of low-temperature expansion in successively larger local clusters or fragments of the allowed zero-temperature states. In principle one need have no *a priori* knowledge of the symmetry of the zero-temperature state. However, there results a packing problem that involves maximizing the number of clusters with optimal free-energy density. In some cases we have been able to solve this problem, while for other parts of the phase diagram we have made conjectures that have yet to be confirmed by rigorous calculations.

I. INTRODUCTION

The technique of low-temperature expansion is a general and rather powerful technique that can be used to reliably construct the low-temperature phase diagram of an Ising lattice model. Although it remains an open problem to establish the conditions for convergence of the low-temperature expansion of arbitrary Ising models, some progress has been made in this direction.¹ In particular, wherever the Pirogov-Sinai theory applies, we are assured that, providing there is only a finite number of zero-temperature states, the low-temperature expansion converges and produces as many phases at finite temperature as there were ground states.² For much of the phase diagram for the present model, we are at present unable to prove one of the conditions which would render the Pirogov-Sinai theory applicable to our study.³ This remains an open and interesting problem for a number of Ising models which possess an infinite number of ground states.

In fact, we have not been able to make very general statements about the applicability of the Peierls-Pirogov-Sinai condition to certain regions of the zero-temperature phase diagram of the present model. This condition would bound the number of low-energy excitations of the zero-temperature states of the model by requiring that the excitation energy scale with the extent of the surface dividing that excitation from the remainder of the zero-temperature state. For such situations one can develop a contour model with convergent low-temperature expansions. The essential content of this procedure is that fluctuations around the zero-temperature state can be de-

scribed as a dilute gas of contours of sufficiently low activity that fluctuations cannot destroy the order of the underlying ground state. In these cases it is appropriate to derive the low-temperature expansions for each of the degenerate zero-temperature states, and then to construct the phase diagram by comparing the free energies of each such state.

An early work on the axial-next-nearest-neighbor interaction (ANNNI) model⁴ due to Fisher and Selke⁵ resulted in a rather complete picture of the low-temperature phase diagram of that model. In their work it was argued that the low-temperature expansion was likely to converge, and later Dinaburg and Sinai were able to rigorously establish convergence for that part of the parameter space studied by Fisher and Selke. The complete low-temperature analysis in Ref. 5 is consistent with results from numerous other studies.⁶

The model we study is defined by the Hamiltonian,

$$\mathcal{H} = -J \sum_{nn'}^{(NN)} \sigma_n \sigma_{n'} - \gamma M \sum_{nn'}^{(DN)} \sigma_n \sigma_{n'} - M \sum_{nn'}^{(LNN)} \sigma_n \sigma_{n'}, \quad (1.1)$$

where the three sums are, respectively, over nearest-, second-nearest-(diagonal), and third-nearest-(axial or linear) neighbor sites on a simple cubic lattice. Notice that the couplings are spatially isotropic so the Hamiltonian transforms according to the full symmetry group of the cubic lattice. This distinguishes it from the ANNNI model which has anisotropic interactions. We mention this important distinction because, although for

some parts of parameter space the zero-temperature states are the same as for the ANNNI model, one expects the fluctuations to be quite different in the two cases. Thus the high symmetry of the Isotropic Hamiltonian is broken spontaneously and the degrees of freedom which ultimately restore the symmetry at higher temperatures, being different from that of the ANNNI model, place the model in a different universality class from an anisotropic model.⁷

For these reasons one must exercise care in applying techniques which have been successful in treating earlier models. In particular, one does not have assurance that the low-temperature series is convergent for all parts of parameter space of the model defined in Eq. (1.1). In what follows we shall assume that it does. Arguments are given to support this proposition.

The plan of the paper is as follows. In Sec. II we reiterate⁸⁻¹⁰ the zero-temperature phase diagram of the lattice model and construct the zero-temperature energy functional in a form appropriate for low-temperature-series expansion. In Sec. III we derive the low-temperature expansion around those parts of the parameter space where the zero-temperature states are highly degenerate. The low-temperature expansion is then used to break this degeneracy, and to evolve the phase diagram for low temperatures.

Finally, in our conclusions to this paper (Sec. IV) we outline those areas of our work on this model which require further research or elucidation. In particular, we discuss some of the weaknesses of present techniques in statistical mechanics when applied to models of the present type.

II. ZERO-TEMPERATURE STATES OF MODEL

The Hamiltonian defined in Eq. (1.1) can be analyzed rather completely in terms of an octahedral cluster of spins consisting of a central, and six surrounding spins. Thus the sum over lattice sites in (1.1) can be replaced with a sum over such clusters of spins. These are independent clusters, and it can be shown that each of them, along with its image obtained by changing the sign of each spin, completely fill a three-dimensional cubic lattice. Thus, if the energy is minimized by one or more of these octahedral clusters of spins, one always has at least one zero-temperature state. If more than one cluster minimizes the energy then one can use a combination of these clusters to completely fill the lattice. In some cases we will see that it is easy to identify, enumerate, and parametrize all such zero-temperature states. In each case such states turn out to be regular or periodic.

As pointed out in Refs. 8-10, and discussed above, it is possible to rewrite the Hamiltonian (1.1) as a sum over the local energy due to octahedral fragments of the cubic lattice. There are ten such independent arrangements of Ising spins surrounding a central plus spin. We designate these clusters and their images under inversion by the symbol C_n^N , where n is the number of spins of a given sign surrounding a central spin of opposite sign and N is the number of these surrounding spins that are coaxial pairs. These spin clusters are shown in Fig. 1. The energy associated with such an octahedral cluster is⁹

$$\begin{aligned} \epsilon_n^N = & -J(3-n) - M[3-2n + N(4-2\gamma)] \\ & - \gamma M(3-n)(2-n). \end{aligned} \quad (2.1)$$

For each choice of J , M , and γ the energy (2.1) is minimized by one or more values of n and N . This information can be presented in the form of a zero-temperature phase diagram, Fig. 1.

The boundaries which appear in Fig. 1 represent the surfaces upon which the energies of the octahedra that are stable on either side are equal. They are given by the formulas

$$J \pm 2M[1 + (3-n)\gamma], \quad m < 0, \quad 0 < \gamma < 2 \quad (2.2)$$

$$J \pm 2M[-1 + (4-n)\gamma], \quad \gamma > 2, \quad n \text{ even} \quad (2.3)$$

$$J \pm 2M[1 + (3-n)\gamma], \quad \gamma > 2, \quad n \text{ odd}. \quad (2.4)$$

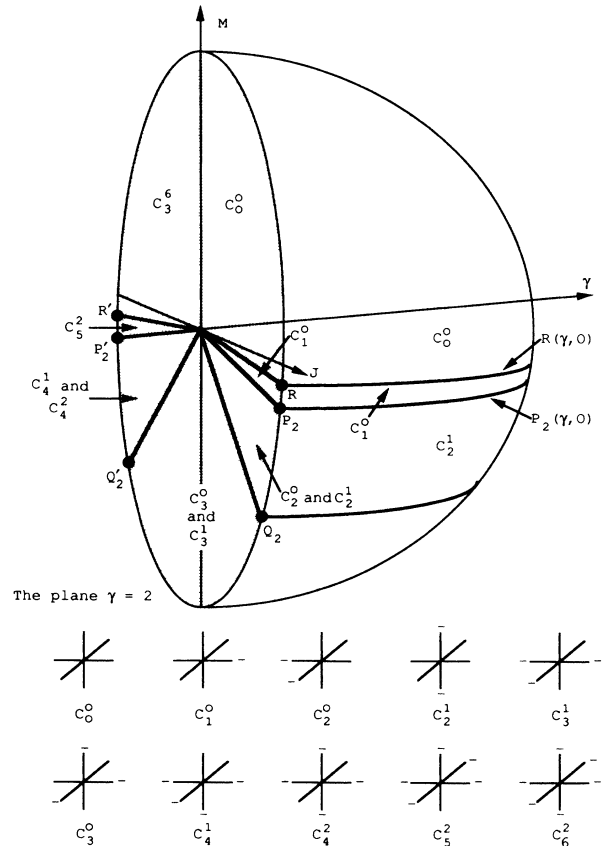


FIG. 1. The zero-temperature phase diagram. In this diagram we illustrate the topology of the zero-temperature-state diagram. Each portion of the diagram is labeled by one or more of the octahedral clusters of spins. These clusters are drawn at the bottom of the figure. Thus, for any choice of J , M and γ one can identify that local cluster, which minimizes the energy density. Typically, along certain surfaces of the zero-temperature-state diagram one has a profound degeneracy in the zero-temperature states. One must resolve this degeneracy using the low-temperature expansion described in the present paper.

Consequently, at any point of the J, M, γ parameter space one can deduce which octahedra minimize the energy and the zero-temperature states can then be constructed by filling the lattice with these and their images under inversion. We now give a description of those regions of the zero-temperature-state diagrams where an infinite number of states is degenerate.

We begin with the surface $R(\gamma, T=0)$ defined by

$$J = -2M(1+2\gamma). \quad (2.5)$$

Along this surface C_0^0 and C_1^0 are degenerate and one can show that from these local configurations it is possible to construct only layered states or the two ferromagnetic ground states. To describe these lamellar states we define s bands, a terminology first introduced by Fisher and Selke⁵ in connection with the ANNNI model. An s band is a sequence of s layers comprised of spins of a given sign, terminated at either end by at least one plane of spins of the opposite sign. Upon examining the ground states along the surface $R(\gamma, T=0)$ one sees that only those layered states without 1 bands are present. If one defines that number of the spins of a given zero-temperature state which belong to s bands to be L_s , then the fraction of such planes will be

$$l_s^r = \frac{L_s^r}{L}, \quad (2.6)$$

which must satisfy the constraints

$$\sum_{s \geq 1}^L s l_s = 1, \quad l_s^r \geq 0. \quad (2.7)$$

Clearly one can define classes of zero-temperature states by assigning a complete set of structural coefficients, $\{l_s^r\}$. This assignment is, of course, not structurally unique unless only one type of s band appears in the structure, or one has more nonlocal information on the sequences of layers in the state. For example, many zero-temperature states have the same fractions of 2 bands and 3 bands. To differentiate between these one would have to assign more complex structural variables such as l_{23} , l_{223} , and so on. However, if any one of these structural variables is unity, then the structure is unique.

It is also clear that in this extended space, the structural variables are no longer independent. Thus the fraction of 23-band sequences, l_{23} , is clearly dependent on the fraction of 2- and 3-band sequences, which satisfy the relation

$$2l_2 + 3l_3 = 1. \quad (2.8)$$

One can write down such relations for general-band-structural variables. However, it will transpire (Sec. III) that, in the vicinity of $R(\gamma, T=0)$ one need consider only the structural variables $l_2, l_3, l_{22}, l_{23}, l_{32}, l_{33}$ in order to resolve the degeneracy between the zero-temperature states. The equations which relate these are, along with Eq. (2.8), given by

$$l_{22} = l_2 - l_{23}, \quad l_{32} = l_{23}, \quad l_{33} = \frac{1}{3} - \frac{2}{3}l_2 - l_{23}. \quad (2.9)$$

Now, since only the local octahedral environments C_0^0

and C_1^0 occur in zero-temperature states along $R(\gamma, 0)$, we need only know the numbers of both types of spin in order to write down the ground-state energy. We define $N^r(C_n^N)$ to be the number of sites of type C_n^N present in the zero-temperature state r . One can then show

$$N^r(C_0^0) = L^2 \sum_{s \geq 3} (s-2)L_s^r, \quad (2.10)$$

$$N^r(C_1^0) = 2L^2 \sum_{s \geq 2} L_s^r. \quad (2.11)$$

Now, using Eq. (2.1) and Eqs. (2.10) and (2.11), we can write the total energy per spin for a zero-temperature state containing no 1 bands as

$$\begin{aligned} \frac{E_L^0}{L^3} [I_s^r, J, M, \gamma] \\ = -3[J + (1+2\gamma)M] + 2[J + 2(1+2\gamma)M] \sum_{s \geq 2} l_s^r. \end{aligned} \quad (2.12)$$

Later on we shall find that a useful parameter in the low-temperature expansion will be

$$\bar{\delta} = J + 2(1+2\gamma)M \quad (2.13)$$

so Eq. (2.12) can be rewritten,

$$\frac{E_L^0}{L^3} = -3\bar{\delta} + 3(1+2\gamma)M + 2\bar{\delta} \sum_{s \geq 2} l_s^r. \quad (2.14)$$

As mentioned earlier, if $\bar{\delta}=0$ one finds that any state which contains no 1 bands is degenerate. If $\bar{\delta}$ is negative, we find $L_s^r=0$ for $s \neq L$ and $l_2 = \frac{1}{2}$. This corresponds to the period-4 layered state or $\langle 2 \rangle$ phase. If $\bar{\delta}$ is positive we find $l_s^r=0$ for $s \neq L$ and $l_L = 1/L$. This solution corresponds to the ferromagnetic phases $\langle \infty \rangle$. This is all the zero-temperature information we need to perform the low-temperature expansion around $R(\gamma, 0)$. This analysis is given beneath Eq. (3.3).

We now return to Eqs. (2.2)–(2.4) and study another degenerate zero-temperature-state manifold. Thus, for $\gamma > 2$ and $n=2$, we obtain from Eq. (2.3) the multistate sheet,

$$J = -2M(-1+2\gamma), \quad (2.15)$$

along which the local octahedra C_0^0 and C_2^1 are degenerate. Again, by inspection one can see that the zero-temperature states are lamellar, and must contain only 1 bands or 2 bands. The structural variables which we require to describe these states are thus l_1, l_2, l_{12}, l_{21} , and so forth. Again, to carry out the low-temperature analysis of Sec. III, we shall need only the following relations:

$$\begin{aligned} l_1 &= l - 2l_2, \quad l_{22} = l_2 - l_{21}, \\ l_{21} &= l_{12}, \\ l_{212} &= l_{12} - l_{112}, \\ l_{112} &= l_{211}. \end{aligned} \quad (2.16)$$

These variables are subject to the constraints

$$\begin{aligned}
0 \leq l_2 \leq \frac{1}{2}, \quad 0 \leq l_{12} \leq \frac{1}{3}, \quad 0 \leq l_{112} \leq \frac{1}{4}, \quad 0 \leq l_{122} \leq \frac{1}{5}, \\
0 \leq 1 - 2l_2 - l_{12} \leq 1, \quad 0 \leq l_2 - l_{12} \leq \frac{1}{2}, \quad 0 \leq l_{12} - l_{122} \leq \frac{1}{3}, \\
l_{12} - l_{112} \leq \frac{1}{3}, \quad 0 \leq l_2 - l_{12} - l_{122} \leq \frac{1}{2}, \quad 0 \leq 1 - l_2 - l_{12} - l_{112} \leq 1.
\end{aligned} \tag{2.17}$$

We can also show that

$$N^r(C_1^0) = L^2 L_2, \tag{2.18}$$

$$N^r(C_1^1) = L^2 L_1, \tag{2.19}$$

and so, using these equations along with Eq. (2.1) and (2.16) we can write the energy for a state r which is constructed only from 1 bands and 2 bands as

$$\frac{E_L^0}{L^3} = \frac{1}{2(2\gamma - 1)} [(5 - 6\gamma)J + (2\gamma - 3)\Delta' + (4 - 8\gamma)\Delta l_2], \tag{2.20}$$

$\gamma > 2$

$$\Delta' = J + (4\gamma - 2)M. \tag{2.21}$$

Note that, as with Eq. (2.14), we have introduced the parameter Δ' which will be important in deriving the low-temperature expansion. We now observe that if $\Delta' > 0$ ($\gamma > 2$) then Eq. (2.20) is minimized by the choice $l_2 = \frac{1}{2}$. If $\Delta' < 0$ we obtain $l_2 = 0$ which, from Eq. (2.16), implies $l_1 = 1$. These situations correspond, respectively, to the period-4 ($\langle 2 \rangle$) and period-2 ($\langle 1 \rangle$) phases. This result is consistent with the zero-temperature-state diagram. We have now succeeded in parametrizing the energy of any state which contains only C_1^0 and C_2^0 spins.

We now turn to the sheet $P_2(\gamma < 2, 0)$, $\gamma > 0$, along which C_1^0 and C_2^0 have equal energies. From Eq. (2.2) we obtain the equation of this surface to be

$$\bar{\eta} = J + 2M(1 + \gamma) = 0 \quad (0 < \gamma < 2). \tag{2.22}$$

Now, these local configurations have the property that they can be combined to construct an infinite number of zero-temperature states, many of which have no periodicity. It is easiest to visualize these states if one defines an interface as the surface which bisects adjacent $+$, $-$ bonds in a given zero-temperature state. All of the states on $P_2(\gamma < 2, 0)$, have translational invariance in one spatial direction. Thus one can treat their construction as the two-dimensional task of piecing together the projections of the C_2^0 and C_1^1 clusters onto the plane. Now, the local octahedron C_1^1 can be used to form flat pieces of interface (or lines in two dimensions) while C_2^0 causes right-angle bends in the interface. The manifold of zero-temperature states is thus comprised of some configurations which have interfaces with right-angle bends at irregular intervals. This makes it remarkably difficult to globally parametrize the manifold using structural variables. However, the energy can still be written as

$$\frac{E_L^0}{L^3} = - \left[N^r(C_1^0) \left[2 - \frac{(2\gamma + 1)}{2(1 + \gamma)} \right] + N^r(C_2^1) \left[1 - \frac{(3 - 2\gamma)}{2(1 + 2\gamma)} \right] \right] J - \left[N^r(C_1^0) \frac{(2\gamma + 1)}{2(1 + \gamma)} + N^r(C_2^1) \frac{(3 - 2\gamma)}{2(1 + \gamma)} \right] \bar{\eta}. \tag{2.23}$$

III. BREAKING THE DEGENERACY USING LOW-TEMPERATURE EXPANSIONS

From the previous section it is evident that there are portions of the parameter space of the Hamiltonian (1.1) where there is an infinity of zero-temperature-states. Our task is to study the fate of these zero-temperature states as the temperature is increased. As mentioned earlier, one expects one of two possible situations. Either this degeneracy will be broken at finite temperature, and then many of the possible states fail to grow into finite temperature phases while the surviving states will evolve to have some finite region of stability in the phase diagram. Alternatively, fluctuations might be so strong that none of the zero-temperature states survives at finite temperature and one then expects the paramagnetic phase to be present in the limit of low temperature. The surface of such points of degeneracy in parameter space would then be a surface of zero-temperature critical points. However, providing one can prove, or perhaps argue, that some sort of Peierls condition exists, we expect the first of these two situations to be applicable.

We now discuss the problems which can arise as a result of having a highly degenerate set of zero-temperature

states. Recall that along the multiphase line $R(\gamma, T=0)$ one can form only layered states. In other parts of the phase diagram two or more octahedral spin clusters are degenerate, and one is then free to compose zero-temperature states with any mixture of them. This again leads to an infinity of states many of them lacking any periodicity. Where the zero-temperature states are layered we can use a low-temperature expansion technique, introduced in Ref. 5, which is based on structural variables, l'_s . In essence this means that we rewrite the free-energy density as a functional of the fraction of short-period sequences occurring in the ground states. One may then seek the global minima of this function for each choice of the coupling parameters. In the absence of underlying periodic structure in the zero-temperature state there appears to be no general procedure for generating the expansion for each such state. In these cases we have chosen to approach the problem differently. Thus we perform low-temperature expansion on small clusters of spins, systematically increasing their size and at each stage removing those which have a higher free-energy density than the rest. This is achieved by first removing those clusters which have higher single-spin-flip energies than the minimal ones. If a number of clusters at the

single-spin excitation level have the same excitation energy then the free energy must be optimized by filling the lattice using the largest concentration of such sites. If there is any remaining degeneracy then one must examine all two-spin-flip clusters occurring in the degenerate manifold and the state which contains the most favorable ones is selected. In principle, one might have to continue this process until the whole lattice is filled. However, in practice one often finds that structural constraints exist on the zero temperature and one-spin-flip manifolds which prevent us from forming arbitrarily large and complicated clusters. One way of seeing this is to recognize that if zero-temperature states are to be built only from two local octahedra then as one builds larger clusters comprised of these two spin configurations, one finds that many avenues are blocked at some cluster size because one would require another type of octahedral spin cluster to continue expanding them. Given the applicability of a Peierls condition we believe this to be a rigorous way to resolve the degeneracy between all types of state existing at zero temperature. In practice, however, it may be difficult to apply because we have no simple systematic way, except by explicit construction, of determining those states which maximize the number of favorable clusters. This is an interesting problem to which, at the minute, we are unable to find a general solution. Nevertheless, one can by laborious construction deduce fairly tight structural constraints on the possible minimal free-energy phases. It is important to note that at least we have replaced the problem of determining finite-temperature phases by a clearly defined packing problem.

A. Curve of degenerate states $R(\gamma, T=0)$

We begin our calculations by constructing the phase diagram in the vicinity of the degeneracy curve $R(\gamma, T=0)$. This study is the least complicated we shall

undertake since the zero-temperature manifold is completely parametrized by structural variables. We have already published a brief description of this calculation⁷ but a fuller account is now given and the calculation extended to higher order.

In Sec. II we showed that, along the curve $R(\gamma, 0)$, one has all layered states which do not contain any 1 bands. This permits us to enumerate all the local environments which can be experienced by a spin in any of the zero-temperature states. These inequivalent sites are labeled $\gamma, o, \tau, \pi, \rho$ and each of them has a distinct excitation energy $\epsilon_\lambda^{(1)}$. The numbers of each type of spin which occur in a zero-temperature state r defined by the set of structural variables $\{l_s\}$ are denoted N_λ^r . These quantities, along with resulting coefficients of the expansion, $a_p^{(1, \alpha, \beta)}$, are collected in Table I. In Table II we collect the same information, but this time for all thirty independent two-spin-flip excitations. Reference 11 contains all the appropriate information for three-spin-flip excitations at $\gamma=2$. The excitation energies $\epsilon^{(1)}\epsilon^{(2)}$ are given for general γ since these two orders are required to completely break the degeneracy. They are calculated in the form

$$\epsilon^{(1)} = \alpha j + \beta \delta, \quad (3.1)$$

$$\epsilon^{(2)} = \alpha' j + \beta' \delta. \quad (3.2)$$

These tables contain all the raw data needed to perform any type of thermodynamic calculation in the vicinity of the curve R .¹² It would probably be worth exploring the rather complete information we have about the zero-temperature states and low-order-expansion coefficients to carefully study such issues as wetting and wetting transitions at finite temperature. These results will be presented in a later paper, but we have taken this opportunity to present all of the data required for such studies.

We begin our present analysis by examining the free-energy density to first order. We have

$$f = \frac{-F}{kTL^3} = \frac{1}{L^3} \ln Z \sim 3\delta - 3(1+2\gamma)m + (-2\delta - 2e^{\epsilon_1} + 2e^{\epsilon_2})l_2 + (-2\delta + 2e^{\epsilon_0} - 3e^{-\epsilon_1} + e^{-\epsilon_4})l_3 \\ + (-2\delta + 2e^{-\epsilon_0} - 4e^{-\epsilon_1} + 2e^{-\epsilon_3}) \sum_{s \geq 4} l_s + e^{-\epsilon_1} \quad (3.3)$$

TABLE I. Excitation energy, degeneracy, and coefficients of expansion for the inequivalent spin sites.

Spin type	ϵ_n	Local configuration	Excitation energy		Degeneracy	$a_0(1, \alpha, \beta)$	$a_2(1, \alpha, \beta)$
			$(1+2\gamma)\alpha$	$(1+2\gamma)\beta$	N		
σ	ϵ_0	+++--	$4(1+3\gamma)$	$4(1+\gamma)$	$2L^2 \sum_{s \geq 3} L_s$	$-\frac{2}{3}$	$\frac{4}{3}$
o	ϵ_1	+++++	$6(1+2\gamma)$	$6(1+2\gamma)$	$L^2 \sum_{s \geq 5} (S-4)L_s$	0	0
τ	ϵ_2	-+++--	$6(1+2\gamma)$	$2(1+2\gamma)$	$2L^2 L_2$	0	-2
π	ϵ_3	++++-	$4(2+3\gamma)$	$4(3\gamma+1)$	$2L^2 \sum_{s \geq 4} L_s$	0	0
ρ	ϵ_4	-+++-	$2(5+6\gamma)$	$2(6\gamma+1)$	$L^2 L_3$	$-\frac{1}{3}$	$\frac{2}{3}$

TABLE II. Energy and coefficients of expansion for the 30 independent two-spin-flip excitations.

Two-spin flip	Excitation energy	$(1+2\gamma)\alpha'$	$(1+2\gamma)\beta'$	$a_0^{(2,\alpha',\beta)}$	$a_2^{(2,\alpha',\beta')}$	$a_{23}^{(2,\alpha',\beta')}$
<i>$\rho\rho$ pairs</i>						
1. Separated	$8[3j+(6\gamma+1)m]$	$20+24\gamma$	$4+24\gamma$	$\frac{13}{6}$	$-\frac{26}{6}$	0
2. in-layer NN	$4[5j+(12\gamma+2)m]$	$16+16\gamma$	$4+24\gamma$	$-\frac{2}{3}$	$\frac{4}{3}$	0
3. in-layer NNN	$4[6j+(12\gamma+1)m]$	$22+24\gamma$	$2+24\gamma$	$-\frac{2}{3}$	$\frac{4}{3}$	0
4. in-layer DN	$4[6j+(11\gamma+2)m]$	$20+26\gamma$	$4+22\gamma$	$-\frac{2}{3}$	$\frac{4}{3}$	0
<i>$\sigma\sigma$ pairs</i>						
1. Separated	$16[j+(\gamma+1)m]$	$8+24\gamma$	$8+8\gamma$	$\frac{19}{3}$	$-\frac{38}{3}$	-5
2. in-layer NN	$4[3j+(4\gamma+4)m]$	$4+16\gamma$	$8+8\gamma$	$-\frac{4}{3}$	$\frac{8}{3}$	0
3. in-layer DN	$4[4j+(3\gamma+4)m]$	$8+26\gamma$	$8+6\gamma$	$-\frac{4}{3}$	$\frac{8}{3}$	0
4. in-layer NNN	$4[4j+(4\gamma+3)m]$	$10+24\gamma$	$6+8\gamma$	$-\frac{4}{3}$	$\frac{8}{3}$	0
5. in-plane NN cross band	$4[5j+(4\gamma+4)m]$	$12+32\gamma$	$8+8\gamma$	$-\frac{1}{3}$	$\frac{2}{3}$	1
6. in-plane NNN in-band	$4[4j+(5\gamma+3)m]$	$10+24\gamma$	$6+8\gamma$	$-\frac{1}{3}$	$\frac{2}{3}$	0
7. in-plane DN cross band	$4[4j+(5\gamma+4)m]$	$8+22\gamma$	$8+10\gamma$	$-\frac{4}{3}$	$\frac{8}{3}$	4
<i>$\tau\tau$ pairs</i>						
1. Separated	$8[2j+(2\gamma+1)m]$	$12+24\gamma$	$4+8\gamma$	0	25	-7
2. in-layer NN	$4[3j+(4\gamma+2)m]$	$8+16\gamma$	$4+8\gamma$	0	-4	0
3. in-layer NNN	$4[4j+(4\gamma+1)m]$	$14+24\gamma$	$2+8\gamma$	0	-4	0
4. in-layer DN	$4[4j+(3\gamma+2)m]$	$12+26\gamma$	$4+6\gamma$	0	-4	0
5. in-plane NN in-band	$4[3j+(4\gamma+2)m]$	$8+16\gamma$	$4+8\gamma$	0	-1	0
6. in-plane NN	$4[5j+(4\gamma+2)m]$	$16+32\gamma$	$4+8\gamma$	0	-1	1
7. in-plane NNN	$4[4j+(4\gamma+3)m]$	$10+24\gamma$	$6+8\gamma$	0	-2	2
8. in-plane DN in-band	$4[4j+(3\gamma+2)m]$	$12+26\gamma$	$4+6\gamma$	0	-4	0
9. in plane DN cross-band	$4[4j+(5\gamma+2)m]$	$12+22\gamma$	$4+10\gamma$	0	-4	4
<i>$\rho\sigma$ pair</i>						
1. Separated	$4[5j+(8\gamma+3)m]$	$14+24\gamma$	$6+16\gamma$	$\frac{12}{3}$	$-\frac{24}{3}$	-2
2. in plane NN in-band	$4[4j+(8\gamma+3)m]$	$10+16\gamma$	$6+16\gamma$	$-\frac{2}{3}$	$\frac{4}{3}$	0
3. in-plane NNN cross-band	$4[5j+(8\gamma+4)m]$	$12+24\gamma$	$8+16\gamma$	$-\frac{2}{3}$	$\frac{4}{3}$	2

TABLE II. (Continued).

Two-spin flip	Excitation energy	$(1+2\gamma)\alpha'$	$(1+2\gamma)\beta'$	$a_0^{(2,\alpha',\beta)}$	$a_2^{(2,\alpha',\beta')}$	$a_{23}^{(2,\alpha',\beta')}$
4. in-plane DN	$4[5j+(7\gamma+3)m]$	$14+26\gamma$	$6+14\gamma$	$-\frac{8}{3}$	$\frac{16}{3}$	0
$\rho\tau$ pair						
1. Separated	$4[5j+(8\gamma+2)m]$	$16+24\gamma$	$4+16\gamma$	0	0	2
2. in plane NNN cross band	$4[5j+(8\gamma+3)m]$	$14+24\gamma$	$6+16\gamma$	0	0	-2
$\sigma\tau$ pair						
1. Separated	$4[4j+(4\gamma+3)m]$	$10+24\gamma$	$6+8\gamma$	0	0	12
2. in plane NN cross-band	$4[5j+(4\gamma+3)m]$	$14+32\gamma$	$6+8\gamma$	0	0	-2
3. in plane NNN cross-band	$6[j+(\gamma+1)m]$	$8+24\gamma$	$8+8\gamma$	0	0	-2
4. in-plane DN	$4[4j+(5\gamma+3)m]$	$10+22\gamma$	$6+10\gamma$	0	0	-8

By examining column 3 of Table I we can see that, in the limit of low temperature, and along the curve $R(\gamma, T=0)$, one can always neglect ε_3 and ε_4 compared to the other terms. One then need consider only the three coefficients of the structural variables,

$$-2(\delta - e^{-\varepsilon_2} + e^{-\varepsilon_1})l_2, \quad (3.4)$$

$$-2(\delta - e^{-\varepsilon_0} + \frac{3}{2}e^{-\varepsilon_1})l_3, \quad (3.5)$$

$$-2(\delta - e^{-\varepsilon_0} + 2e^{-\varepsilon_1}) \sum_{s \geq 4} l_s, \quad (3.6)$$

by expanding the exponentials in Eq. (3.3) one can see that for $\delta \geq 0$, the coefficients of l_3 and $\sum_{s \geq 4} l_s$ are dominant. Furthermore, from Eqs. (3.5) and (3.6) one can decide whether the coefficients of the structural variables are positive or negative. If the coefficient of l_3 is positive then the coefficient of $\sum_{s \geq 4} l_s$ will be less positive. Consequently it is more favorable to maximize l_3 .

On the other hand, if the coefficient of the 3-band structural variable is negative (for $\delta > 0$) then it is more favorable to minimize the sum $\sum_{s \geq 4} l_s$. In a large cubic system of side L the coefficient $l_\infty = 1/L$ is the minimal structural variable. Thus, for $\delta > 0$ and infinite system size ($L \rightarrow \infty$), we find the period -6 or $\langle 3 \rangle$ phases to be in equilibrium with the $\langle \infty \rangle$ phase along the coexistence curve,

$$\delta_{3,\infty}^{(1)} = e^{-\varepsilon_0} - \frac{3}{2}e^{-\varepsilon_1}. \quad (3.7)$$

One can see that it is not possible to mix L sequences and 3 sequences to make a new phase which is stable along this boundary. In addition (see Sec. IV), the surface tension between $\langle \infty \rangle$ and $\langle 3 \rangle$ can be shown to be positive along the curve (3.7). Clearly Eq. (3.7) represents a curve

of first-order phase transitions between $\langle 3 \rangle$ and $\langle \infty \rangle$ phases. However, if $\delta > 0$ the situation is more complicated. By examining Eqs. (3.4) and (3.5) one can see that there is a locus where the free-energy-density of 2 bands and 3 bands is equal:

$$\delta_{2,3} = -2e^{-\varepsilon_0} + 3e^{-\varepsilon_2} - e^{-\varepsilon_4}. \quad (3.8)$$

Now it is possible to construct an infinite number of phases comprised only of 2 bands and 3 bands which, along the curve (3.8), have degenerate free-energy density. Clearly we must proceed to higher order in the spin-flip calculation in order to resolve this degeneracy. However, our task is now somewhat easier since we now need to consider those states which contain only 2 bands and 3 bands. Thus, in Table II, we have presented all the information required to write the free-energy functional to second order. As pointed out in Sec. II, we are able to eliminate all but the structural variables of 2- and 3-band sequences in the free-energy density contributions, $\Delta f^{(n)}$, arising from the n th-order spin-flip analysis,

$$f = -\frac{F}{L^3 kT} = \sum_{n=0} \Delta f^{(n)} \sim \Delta f^{(0)} + \Delta f^{(1)} + \Delta f^{(2)}, \quad (3.9)$$

$$\Delta f^{(0)} = -3(1+2\gamma)m + 2\frac{1}{3}\delta - \frac{2}{3}\delta l_2, \quad (3.10)$$

$$\Delta f^{(f)} = -\sum_{\alpha,\beta} \sum_p a_p^{(1,\alpha,\beta)} l_p x^\alpha y^\beta, \quad (3.11)$$

$$\Delta f^{(2)} = -\sum_{\alpha',\beta'} \sum_p a_p^{(2,\alpha',\beta')} l_p x^\alpha y^{\beta'}, \quad (3.12)$$

where the coefficients $a_p^{(n,\alpha,\beta)}$ can be read from Tables I and II. One now has the free-energy-density for any J , γ , and δ as a linear functional only of l_2 and l_{23} subject to the constraints [see Eqs. (2.8) and (2.9)]

$$\begin{aligned}
l_2 &\geq 0, \quad l_3 = \frac{1}{3} - \frac{2}{3}l_2 \geq 0 \quad \text{or} \quad l_2 \leq \frac{1}{2}, \\
l_{23} &\geq 0, \quad l_{22} = l_2 - l_{23} \geq 0, \\
l_{33} &= \frac{1}{3} - \frac{2}{3}l_2 - l_{23} \geq 0.
\end{aligned} \tag{3.13}$$

As Fisher and Selke pointed out, the task of minimizing (3.9) subject to constraints (3.13) is a standard linear programming task. Indeed, at each order of the low-temperature expansion one will find that one has a higher-dimensional linear programming problem. The appropriate extensions of the inequalities (3.13) form a convex polytope \mathcal{P}_n in the space of the structural variables. Generally one expects to find that the extremum of the functional lies on a unique vertex of the convex polytope \mathcal{P}_n . However, the location of the vertices of a convex polytope may in itself be a nontrivial problem. For the structural space defined in (3.13) the polytope is two dimensional and Fisher and Selke have found the vertices to be

$$(l_2, l_{23}) = (0, 0), \quad \langle 3 \rangle \tag{3.14}$$

$$= (\frac{1}{5}, \frac{1}{5}), \quad \langle 23 \rangle \tag{3.15}$$

$$= (\frac{1}{2}, 0), \quad \langle 2 \rangle \tag{3.16}$$

where, using the definitions in (2.16), we have also marked the thermodynamic phase corresponding to that vertex of the polytope.

We must now check explicitly to see whether the free energy is optimized at these vertices and to do this we again appeal to an argument given in Ref. 5. One of the vertices of the polytope, Eq. (3.15), represents a new phase, ($\langle 23 \rangle$), which was not resolved in the first-order calculation. We are now interested in the possibility that it can appear along the curve which defines the equality of free-energy density between $\langle 3 \rangle$ and $\langle 2 \rangle$ phases. By using the values of l_2 and l_{23} for the $\langle 2 \rangle$ and $\langle 3 \rangle$ phases in the equation for free-energy-density, Eq. (3.9), we find the condition that the coefficient of the 2-band structural variable must vanish. Consequently, along the curve defined by this condition, the free-energy-density will be optimized by that choice which maximizes the term in the 23-band structural variable.

The reader may now make reference to Table II, where one sees that the coefficient of the leading l_{23} term is positive. This means that its contribution to the functional (3.9) is negative. Consequently, the functional (3.9) is optimized when $l_{23} = 0$, that is, it is never favorable to have 23 bands present in a thermodynamic phase along curve

(3.8). We conclude that only three distinct thermodynamic phases arise from the curve $R(\gamma, 0)$. Note that there are a number of potential weaknesses in the arguments above. For example, it is expected, but not certain, that the extremae of the linear functional defined on the convex polytope are simply the vertices of that polytope. We have attempted to check our conclusions numerically and have obtained the same answer as above. However, given the rather unfamiliar nature of the model and the rather remarkable conclusions implied by the above analysis it is probably worth seeking more rigorous justification of the linear programming analysis.

The above results for the surfaces of infinitely degenerate zero-temperature states $R(\gamma, 0)$, $(\gamma, 0)$ ($\gamma > 2$) are remarkable. They indicate that in each case only one out of a large number of degenerate zero-temperature states is stable at finite temperature. In the ANNNI model one has the same zero-temperature manifold as at $R(\gamma, 0)$. In that case, however, an infinite number of phases spring from the degeneracy and one then speaks of a multiphase point. Furthermore, the mean-field theory is known to break the degeneracy at the ANNNI multiphase point correctly. In the present isotropic model this is not the case. The ferromagnetic and $\langle 3 \rangle$ phases are well described by mean-field theory, but one predicts in addition many other layered phases which are precluded by a second-order low-temperature analysis.

The conclusions of our present analysis are clear. In the region defined by $R(\gamma, T)$, with T small, we have only four phases. There are the positive and negative magnetized ferromagnetic phases (which are in first-order coexistence with the $\langle 3 \rangle$ phase) and the $\langle 2 \rangle$ phase which also has a first-order boundary with the $\langle 3 \rangle$ -phase. In Ref. 11 we extend the above analysis to third order in spin flips.

We now turn to a calculation which elucidates the phase structure around $P_2(\gamma, T=0)$. Although the calculation is different from the one above, the basic strategy is the same as we have already used.

B. Curve of degenerate states $P_2(\gamma, 0)$; $\gamma > 2$

The curve $P_2(\gamma, 0)$ is another of the important regions of parameter space where there is a high degree of degeneracy of the zero-temperature states. The situation at $\gamma = 2$, that is at the point $P_2(2, 0)$, is complicated and we return to this matter later in this section (Sec. III C). For $\gamma > 2$ the zero-temperature states are composed only of

TABLE III. Single-spin-flip excitation energies for the curve $P_2(\gamma > 2, 0)$.

Type of excitation	ϵ_n	Excitation energy		Degeneracy N
		$(2\gamma - 1)\alpha$	$(2\gamma - 1)\beta$	
a: + - + - +	ϵ_0	$12\gamma - 10$	$6 - 4\gamma$	$L_{111}L^2$
b: - - + + -	ϵ_1	$12\gamma - 10$	$2 + 4\gamma$	$2L_{22}L^2$
c: - + + - +	ϵ_2	$12\gamma - 12$	$4 + 4\gamma$	$2L_{12}L^2$
d: + + - + -	ϵ_3	$12\gamma - 8$	$4 - 4\gamma$	$2L_{211}L^2$
e: + + - + +	ϵ_4	$12\gamma - 6$	$2 - 4\gamma$	$L_{212}L^2$

TABLE IV. Data for two-spin-flip calculation.

	a_0	a_2	a_{12}	a_{112}	a_{122}	a_{1112}	a_{1122}	a_{1212}	a_{1222}	a_{11112}	$(2\gamma-1)\alpha$	$(2\gamma-1)\beta$
<i>aa pair</i>												
1. Separated	$\frac{25}{2}$	-24	$-\frac{25}{2}$	$-\frac{25}{2}$		-6				-1	$-20+24\gamma$	$12-8\gamma$
2. NN in layer	-2	+4	+2	+2							$-16+16\gamma$	$12-8\gamma$
3. 2NN in layer	-2	+4	+2	+2							$-18+24\gamma$	$10-8\gamma$
4. diag. in layer	-2	+4	+2	+2							$-20+26\gamma$	$12-10\gamma$
5. NN,IP,CB	-1	+1	+1	+1		+1					$-24+32\gamma$	$12-8\gamma$
6. NN,IP,C2BS	-1	+2	+1	+1		+1				+1	$-18+24\gamma$	$10-8\gamma$
7. diag,IP,CB	-4	+8	+4	+4		+4					$-20+22\gamma$	$12-6\gamma$
<i>bb pair</i>												
1. Separated		25	-25		-7						$-20+24\gamma$	$4+8\gamma$
2. NN,IL		-4	+4								$-16+16\gamma$	$4+8\gamma$
3. 2NN,IL		-4	+4								$-18+24\gamma$	$2+8\gamma$
4. diag,IL		-4	+4								$-20+26\gamma$	$4+6\gamma$
5. NN,IP,IB		-1	+1		+1						$-16+16\gamma$	$4+8\gamma$
6. NN,IP,CB		-1	+1								$-24+32\gamma$	$4+8\gamma$
7. 2NN,IP,CB		-2	+2		+2						$-22+24\gamma$	$6+8\gamma$
8. diag,IP,IB		-4	+4		+4						$-20+26\gamma$	$4+6\gamma$
9. diag,IP,CB		-4	+4								$-20+22\gamma$	$4+10\gamma$
<i>cc pair</i>												
1. Separated			+18		-5						$-24+24\gamma$	$8+8\gamma$
2. NN,IL			-4								$-20+16\gamma$	$8+8\gamma$
3. 2NN,IL			-4								$-22+24\gamma$	$6+8\gamma$
4. diag,IL			-4								$-24+26\gamma$	$8+6\gamma$
5. NN,IP,IB			-1		+1						$-20+16\gamma$	$8+8\gamma$
6. diag,IP,IB			-4		+4						$-24+26\gamma$	$8+6\gamma$
<i>dd pair</i>												
1. Separated				19		-6					$-16+24\gamma$	$8-8\gamma$
2. NN,IL				-4							$-12+16\gamma$	$8-8\gamma$
3. 2 NN,IL				-4							$-14+24\gamma$	$6-8\gamma$
4. diag,IL				-4							$-16+26\gamma$	$8-10\gamma$
5. NN,IP,CB				-1		+1					$-20+32\gamma$	$8-8\gamma$
6. NN,IP,C2BS				-1		+1					$-14+24\gamma$	$6-8\gamma$
7. diag,IP,CB				-4		+4					$-16+22\gamma$	$8-6\gamma$
<i>ee pair</i>												
1. Separated			$\frac{13}{2}$	$-\frac{13}{2}$							$-12+24\gamma$	$4-8\gamma$
2. NN,IL			-2	+2							$-8+16\gamma$	$4-8\gamma$
3. 2NN,IL			-2	+2							$-10+24\gamma$	$2-8\gamma$
4. diag,IL			-2	+2							$-12+26\gamma$	$4-10\gamma$
<i>ab pair</i>												
1. Separated											$-20+24\gamma$	8
<i>a,c pair</i>												
1. Separated						2					$-22+24\gamma$	10
2. NN,IL						-2					$-20+24\gamma$	8

TABLE IV. (Continued).

	a_0	a_2	a_{12}	a_{112}	a_{122}	a_{1112}	a_{1122}	a_{1212}	a_{1222}	a_{11112}	$(2\gamma-1)\alpha$	$(2\gamma-1)\beta$
<i>ad</i> pair												
1. Separated						10				2	$-18+24\gamma$	$10-8\gamma$
2. NN,IP,CD						-2					$-22+32\gamma$	$10-8\gamma$
3. 2NN,IP,C2BS										-2	$-16+24\gamma$	$8-8\gamma$
4. diag,IL						-8					$-18+22\gamma$	$10-6\gamma$
<i>ae</i> pair												
1. Separated											$-16+24\gamma$	$8-8\gamma$
<i>bc</i> pair												
1. Separated					12						$-22+24\gamma$	$6+8\gamma$
2. NN,IP,IB					-2						$-18+16\gamma$	$6+8\gamma$
3. NN,IP,CB					-2						$-24+24\gamma$	$8+8\gamma$
4. diag,IP,IB					-8						$-22+26\gamma$	$6+6\gamma$
<i>bd</i> pair												
1. Separated								+2			$-18+24\gamma$	6
2. 2NN,IP,CB								-2			$-20+24$	8
<i>be</i> pair												
1. Separated			+1	-1	+1			-1	-1		$-16+24\gamma$	4
2. 2NN,IP,CB			-1	+1	-1			+1	+1		$-18+24\gamma$	6
<i>cd</i> pair												
1. Separated			1	13	-1	-2	-1	-1			$-20+24\gamma$	8
2. NN,IP,CB				-2							$-24+32\gamma$	8
3. 2NN,IP,CB			-1	-1	+1		+1	+1			$-22+24\gamma$	10
4. 2NN,IP,C2BS				-2		+2					$-18+24\gamma$	6
5. diag,IP,CB				-8							$-20+22\gamma$	$8+2\gamma$
<i>ce</i> pair												
1. Separated			12	-12	-2			2			$-18+24\gamma$	6
2. NN,IP,CB			-2	+2							$-22+32\gamma$	6
3. 2NN,IP,CB			-2	+2	+2		-2				$-20+24\gamma$	8
4. diag.,IP,CB			-8	+8							$-18+22\gamma$	$6+2\gamma$
<i>de</i> pair												
1. Separated											$-14+24\gamma$	$6-8\gamma$

C_1^0 and C_2^1 and we are free to make only layered phases with 1 bands and 2 bands. This means that the method of structural variables can be used to study the problem. The only difference will be that our analysis is based on different structural variables, l_1 , l_2 , l_{21} , l_{221} , l_{112} , and so on.

The single-spin-flip excitation energies for the curve $P_2(\gamma > 2,0)$ are given in Table III. Table IV contains all the relevant data for the two-spin-flip calculation.

Note that the structural coefficients in column three of Table III are not all independent. They are related by Eq. (2.16). There are, in fact, only three independent structural coefficients at this order of the expansion. Similarly, the structural coefficients in Table IV can be reduced to a minimal set.

From Eq. (2.20) and the information in Table I we can construct the free energy density up to the one-spin-flip level. The result is

$$f \sim \Delta f^{(0)} + \Delta f^{(1)} = [-1/(4\gamma - 2)][(5 - 6\gamma)j + (2\gamma - 3)\Delta] - e^{-\varepsilon_1} + (2\Delta - 2e^{-\varepsilon_1} + 2e^{-\varepsilon_2})l_2 \\ + (2e^{-\varepsilon_0} - e^{-\varepsilon_1} - 2e^{-\varepsilon_2} + e^{-\varepsilon_4})l_{12} + (-e^{-\varepsilon_1} + 2e^{-\varepsilon_3} - e^{-\varepsilon_4})l_{112} \\ (\gamma > 2 \text{ and } \Delta = \Delta^1/kT). \quad (3.17)$$

Now, if Δ is positive it is clear that the functional is maximized by the choice $l_2 = \frac{1}{2}$ and one obtains the $\langle 2 \rangle$ phase. If Δ is negative we have $l_2 = 0$ which then implies the $\langle 1 \rangle$ phase.

As for the previous analysis, to proceed to higher order we must now construct the convex polytope from the structural variables $l_2, l_{12}, l_{112}, l_{122}$, constrained by Eqs. (2.17). The vertices of this polytope correspond to the states which may be stabilized at second order in the spin-flip calculation. The linear programming analysis was carried out by taking all possible linear combinations of the structural variables with coefficients 0, +1. This procedure, while usually reliable, can result in vertices being missed, but we have attempted to check our results in various ways. The six vertices are given in Table V and we have also marked the thermodynamic phase to which they correspond.

Now consider the locus defined by the equality of the free-energy-density of $\langle 1 \rangle$ and $\langle 2 \rangle$ phases,

$$\Delta^{(1)} \sim e^{-\varepsilon_1} - e^{-\varepsilon_2}. \quad (3.18)$$

We see that the coefficient of the structural variable for 2 bands vanishes and consequently the free-energy density need be optimized only with respect to l_{12} and l_{112} . Now, at low temperature the leading term in the coefficients of these variables is the exponential of ε_0 and, since this gives a positive contribution, we can see that it is more favorable to maximize l_{12} than l_{112} . Thus along the curve (3.18) the $\langle 21 \rangle$ phase is more stable than the $\langle 211 \rangle$ phase.

The two other pseudoequilibria which must be examined are as follows. The curve along with the $\langle 2 \rangle$ and $\langle 21 \rangle$ phases have the same free-energy density [Eq. (3.19)],

$$\Delta_{2,12}^{(1)} = 2e^{-\varepsilon_0} + e^{-\varepsilon_4}, \quad (3.19)$$

and also curve (3.20),

$$\Delta_{1,21}^{(1)} = -e^{-\varepsilon_0} + \frac{3}{2}e^{-\varepsilon_1} - \frac{1}{2}e^{-\varepsilon_4}, \quad (3.20)$$

along which the $\langle 1 \rangle$ and $\langle 21 \rangle$ phases have equal free-energy density. These are regions where new phases may be stabilized at second order in our calculations.

Now along the curve (3.19) we find that the phase $\langle 221 \rangle$ has equal free energy to the $\langle 2 \rangle$ and $\langle 21 \rangle$ phases. Consequently one must proceed to higher order to resolve this degeneracy.

However, along the curve (3.20) one finds that the free-energy density of the $\langle 211 \rangle$ phase is higher than that of the $\langle 1 \rangle$ or $\langle 21 \rangle$ phases. We therefore conclude that no new phase can appear between the $\langle 1 \rangle$ and $\langle 21 \rangle$ phases when the temperature is very low.

Now, by an argument similar to that around Eqs. (3.9)–(3.12) we can show that, along the locus defined by the equality of the free energy density of $\langle 2 \rangle$ and $\langle 21 \rangle$ phases, one need only consider the leading behavior of the coefficient of the structural variable l_{221} . By consulting Table IV one finds that the excitation energy for the nearest-neighbor, in-plane, in-band pair of spins is the lowest for all $\gamma > 2$.

The coefficient from Table IV is positive, so it is never favorable to make l_{221} nonzero. We conclude, therefore, that the $\langle 2^21 \rangle$ phase is not stable in the vicinity of $P_2(\gamma, 0)$ for $\gamma > 2$.

The topology of the phase diagram in this region is quite similar to that around $R(\gamma, 0)$. Thus, at low temperatures, one has the $\langle 2 \rangle$ phase for Δ positive while for Δ negative the $\langle 1 \rangle$ phase is favored. Between these two phases there arises a third, the $\langle 21 \rangle$ phase, which it may be shown, is separated from them by first-order phase transitions.

C. Point of degenerate states $P_2(\gamma, 0)$; $\gamma < 2$

We next turn to the low-temperature analysis along the sheet $P_2(\gamma, 0)$ ($0 < \gamma < 2$). Recall from Sec. II that the zero-temperature states are complex, many being aperiodic in two of the three lattice directions. The energy of these states depends only on the number of C_1^0 and C_2^1 spins and is given by Eq. (2.23). As pointed out at the beginning of Sec. III, although we no longer have any structural variables one can still solve that part of the problem which involves resolving between different free-energy densities. In principle, this involves the systematic construction of all one-spin-flip clusters¹³ which can be composed from the allowed local octahedra. One then deduces which of these have the lowest one-spin-flip energy. This is a straightforward if tedious task. However, the second part of the problem is more difficult to solve. Using the optimal one-spin-flip cluster or clusters one must construct that complete filling of the lattice which maximizes the number of optimal clusters subject to the constraint that the zero-temperature energy be minimal.

TABLE V. Structural variables for the six vertices, including the thermodynamic phase.

Vertex	l_2	l_{12}	l_{112}	l_{122}	phase
1	0	0	0	0	$\langle 1 \rangle$
2	$\frac{1}{2}$	0	0	0	$\langle 2 \rangle$
3	$\frac{1}{3}$	$\frac{1}{3}$	0	0	$\langle 12 \rangle$
4	$\frac{1}{4}$	$\frac{1}{4}$	$\frac{1}{4}$	0	$\langle 112 \rangle$
5	$\frac{2}{5}$	$\frac{1}{5}$	0	$\frac{1}{5}$	$\langle 122 \rangle$
6	$\frac{1}{3}$	$\frac{1}{6}$	$\frac{1}{6}$	$\frac{1}{6}$	$\langle 1122 \rangle$

Thus, the zero-temperature energy may be written as a linear combination of terms from high-energy sites, these having optimal one-spin-flip energies, and low-energy sites which have the least favorable spin-flip energies. For a fixed total ground-state energy this arrangement yields the maximum number of favorable one-spin-flip excitations in a structure. However, it may not be possible to form a phase with these fractions of different sites and the construction must be generalized somewhat. Alternatively, it may be possible to make more than one phase with the appropriate fraction of high- and low-energy sites.

The first problem is in principle resolvable by introducing some sites which have the next highest site energy. The introduction of such sites will also force us to reduce the number of optimal one-spin-flip clusters, but if they permit complete tiling of the lattice then providing the state so formed is unique it will be the thermodynamic phase.

If at any stage of this construction it is possible to form more than one structure which conforms to the constraints implied by the ground-state energy then one must examine each of these phases at the two-spin-flip level. The procedure is analogous to the one described above, that is, we maximize the number of optimal two-spin-flip clusters subject to the fixed ratio of one-spin-flip clusters.

This procedure is in principle exact and would permit us to resolve the degeneracy of the zero-temperature state manifold of any regular Hamiltonian. In our experience the main challenge in carrying out the construction is of a geometrical nature since it may be difficult to find a tiled lattice configuration with a fixed fraction of local clusters.

In the present case, that is, along the sheet $P_2(\gamma, 0)$, $\gamma < 2$, we have only C_1^0 and C_2^1 local octahedra available to us. However, there are infinitely many zero-temperature states which can be formed from these sites, so we begin constructing all possible one-spin-flip clusters with these octahedra and decide which are optimal.

There may be shortcuts to the construction of the optimal one-spin-flip cluster.

In the present case one finds that the optimal one-spin-flip clusters are those given below, in Figs. 2(a) and 2(b). Now the thermodynamically favored state in this region is that phase which contains the maximal number

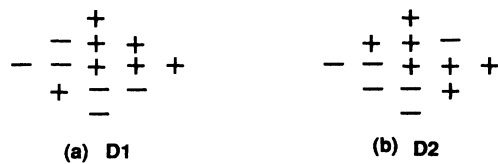


FIG. 2. The x - y projections of the two optimal one-spin-flip clusters (D1 and D2) in the region $P_2(\gamma, 0)$, $\gamma < 2$. All zero-temperature states are translationally invariant in one of the three spatial directions so one need only present information on the planar projections of the states and clusters.

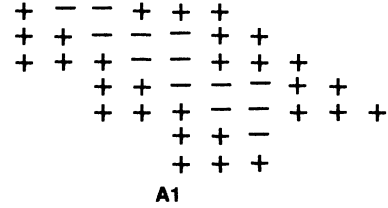


FIG. 3. Here we present the best solution we have been able to find to the problem of maximizing the number of optimal clusters [D1 and D2 of Figs. 2(a) and 2(b)] present in a phase. The structure exhibited here has translational invariance in the third direction.

of spin-flip clusters D1 and D2, and is comprised only of local octahedra C_1^0 and C_2^0 .

We first note that the zero-temperature energy can be equally well described in terms of the clusters C_n^N or the single-spin-flip clusters. For practical purposes we have always chosen to construct the zero-temperature states using the octahedral clusters, C_n^N , since this is a simpler task. However, the argument which follows shows that if one is dealing with the problem of optimally packing space with the clusters in Fig. 2 it may be helpful to consider zero-temperature states as being comprised of the more extended clusters D1 and D2.

Now to each of the clusters in Fig. 2, one can assign a local energy, the total energy of the state being given by

$$E_L^0 = \sum_i N_i E_{ex}^i, \quad (3.21)$$

where N_i is the number of single-spin-flip cluster of type i and E_{ex}^i is the energy of extended cluster.

The total energy calculated from both equations must, of course, be the same. Also we know that the extended cluster with the highest site energy results in the lowest single-spin-flip-excitation energy. Thus, since the optimal thermodynamic state is constructed by using as many low-energy-excitation clusters as possible, one expects that it is more favorable to use these in conjunction with the highest-energy-excitation (or lowest ground-state) energy clusters. Using only these extreme clusters one hopes to optimize the number of favorable ones. The best phase we have been able to construct (A1) is illustrated in Fig. 3. In this instance it is possible that another phase with a larger number of optimal single-spin-flip clusters does exist.

D. Point of degeneracy, $P_2(\gamma=2, 0)$

We next turn to the special point on the zero-temperature diagram, $P_2(2, 0)$. From Eq. (2.1) and (2.15) one finds that there are three degenerate octahedral clusters C_1^0 , C_2^0 , and C_2^1 at this point. Consequently, there are many new zero-temperature states at $P_2(2, 0)$ which could not be formed along $P_2(\gamma, 0)$ for $\gamma > 2$. We now analyze the phase behavior at finite temperature using the same argument as that given in the previous section. Thus the local environment with the highest spin-site energy has the lowest one-spin-flip energy. In the present case we

find that there are six degenerate one-spin-flip energies ($\epsilon_1 = 10/3j$). The clusters $D3-D9$ to which they correspond are shown in Figs. 4(a)–4(f). In Fig. 4(g) we illustrate that cluster which has the highest one-spin-flip energy ($\epsilon = -20/3j$) and consequently the lowest ground-state site energy.

Now, as before, one expects that the thermodynamically favored phases are constructed by using as many of the optimum clusters [Figs. 4(a)–4(e)] in conjunction with the lowest site energy cluster [Fig. 4(g)]. We require that the total energy per spin be $-\frac{7}{6}j$, a result which one can obtain from Eqs. (2.1) and (2.15) with the value $\gamma = 2$. We now wish to determine that largest fraction of optimal spin-flip cluster, b , and lowest extended site energy cluster which satisfies the equation for the zero-temperature energy:

$$\frac{-\frac{5}{6}j + b(-\frac{10}{6})j}{1+b} = -\frac{7}{6}j. \quad (3.22)$$

This equation has the solution $b = \frac{2}{3}$. Consequently, the favored thermodynamic phases will have three optimal one-spin-flip clusters to every two low-ground-state-energy clusters. The maximal multiplicity that the optimal spin-flip clusters can achieve is $\frac{3}{5}L^3$. Note, however, that we have no *a priori* reason to suppose that a state with this multiplicity is unique, though we believe it to be so.

If the phase was not unique then our present strategy could still, in principle, be made exact. This would entail collection of all those structures which are comprised of $\frac{3}{5}L^3$ optimal spin-flip clusters and $\frac{2}{5}L^3$ minimal ground-state-energy clusters. One would then check to see which of these phases contain optimal two-spin-flip clusters. If there is more than one such state then the degeneracy would be resolved by establishing which state contains the maximum number of optimal-two-spin-flip clusters. As mentioned at the beginning of this section, this procedure could be continued until one reaches sufficiently extended spin-flip clusters which remove all degeneracies that are not rigorous consequences of the Hamiltonian itself.

However, in the present case we believe the phase ($A2$) shown in Fig. 5 to be an equilibrium one. The complete resolution of such issues must await better understanding of how to achieve optimal packing of a small number of specified clusters.

We now pause to review what thus so far been achieved by our analysis. The low-temperature phase diagram in the region of $R(\gamma, 0)$, $P_2(\gamma, 0)$, $P_2(2, 0)$ has been constructed. In most of the other regions of the zero-temperature-state diagram the zero-temperature states are unique or the degeneracy is a fundamental consequence of the symmetries of the Hamiltonian and persists when fluctuations are included in the analysis. There is, however, one rather difficult region of degeneracy found between the lines $J + 6M = 0$ and $J + 2M = 0$. $\gamma = 2$ in Eq. (2.2), where the clusters C_2^0 and C_2^1 have the same ground-state energy. It transpires that this degeneracy is never broken at finite temperature by mean-field (saddle-point) calculations or even at the one-loop level. Thus

the low-temperature expansion may be the only practicable technique to rigorously study this part of the phase diagram.

E. In the region of degeneracy $P_2Q_2(\Delta, \tau, T=0)$ for $\tau < 0$

As a prelude to our study of the more difficult problem [$P_2Q_2(\Delta, \tau=0, T=0), \tau = \gamma - 2$] we now construct the low-temperature phase diagram near this line of degeneracy, but for $\gamma < 2$.

We shall again use Eq. (2.20) (with $\gamma = 2$) to define an important parameter in the expansion. As before,

$$\Delta = \frac{\Delta'}{kT} = j + 6m. \quad (3.23)$$

We also define the parameter

$$\tau = \gamma - 2. \quad (3.24)$$

It is possible to examine the phase diagram in the vicinity of $P_2Q_2(\Delta, \tau, T=0)$ which is defined as the strip in zero-temperature phase diagram bounded by the lines

$$J + 2M(1 + \gamma) = 0, \quad (3.25)$$

$$J + 2M = 0, \quad (3.26)$$

when $\gamma < 2$, and between the lines,

$$J + 2M(-1 + 2\gamma) \quad (3.27)$$

and Eq. (3.26) when $\gamma \geq 2$.

When $\gamma > 2$ the unique zero-temperature state is the $\langle 1 \rangle$ phase. When $\gamma < 2$ there are only two possible zero-temperature states. These are the $\langle 2:2:\infty \rangle$ phase and $\langle 2:2:\infty \rangle_D$ diagonal phase. We can resolve the degeneracy between these by the argument below.

In brief, the result of that argument will be that the $\langle 2:2:\infty \rangle$ and $\langle 2:2:\infty \rangle_D$ have equal free-energy-densities up to three-spin-flip excitations. At fourth order the degeneracy is broken, and we find that the $\langle 2:2:\infty \rangle$ phase is always favored.

We begin by recalling that the zero-temperature energy can be calculated using either the octahedral clusters C_n^N or the extended (single-spin-flip) clusters D . When the extended clusters are used one usually finds a number of inequivalent site energies in any phase. However, one can show that in the present case both phases have only one type of site energy. This introduces some simplifying features into our arguments. In particular, we know that spin-flip excitations of any order are given by n times the disconnected single-spin-flip energy of a site, minus the contributions from directly coupled bonds in the cluster.

For example, the two-spin-flip energy for nearest-neighbor sites 1,2, is given by

$$\epsilon^2 = 4\epsilon^1 - 4J\sigma_1\sigma_2. \quad (3.28)$$

Since the site energies of both the $\langle 2:2:\infty \rangle$ and $\langle 2:2:\infty \rangle_D$ phases are equal so are their one-spin-flip energies. In turn this means that only the second term in Eq. (3.28) can resolve between two-spin-flip excitations in the two phases. However, since the two phases are constructed from the same octahedral clusters, both must

have the same number of nearest-neighbor bonds of (+, +), (+, -), and (-, -) types. In addition, they also have the same number of diagonal-neighbor and linear-next-nearest-neighbor bonds. The conclusion of this observation is that the two phases have equal numbers of equal excitation energy two-spin-flip clusters. Clearly no degeneracy in thermodynamic states can be resolved up to and including two-spin-flip excitations. For three-spin-flip clusters a similar argument holds. One can actually exhaustively construct all independent triples of spins in the two phases but this is a lengthy task and we merely report the conclusion that there are equal numbers of a given excitation cluster in both phases.

Now proceeding to fourth order in spin-flip excitations

we are able to break this degeneracy in favor of the $\langle 2:2:\infty \rangle$ phase. The argument is a little involved because we do not wish to explicitly construct a table of the multiplicities of all four-spin-flip excitations. It is preferable first to eliminate all clusters which can be seen to have *a priori* equal multiplicities in both phases. The rules which may be formulated to achieve this are as follows.

(a) If the *xy* projection of any four-spin cluster, or for that matter any geometrical *n*-mer, has the same multiplicity in the plane of either of the phases $\langle 2:2:\infty \rangle$ or $\langle 2:2:\infty \rangle_D$, then this cluster will have the same multiplicity in the full three-dimensional zero-temperature state. This argument takes advantage of the translational symmetry found in the *z* direction. The number of dimen-

TABLE VI. Clusters and their excitation energies in terms of *j* and Δ .

Cluster type	1 flip excitation energy		Cluster type	1 flip excitation energy	
	$j + 6m = \Delta$ $-2j < \Delta < 0$	$j + 2m = \bar{\Delta}$ $0 < \bar{\Delta} < 2/3j$		$j + 6m = \Delta$ $-2j < \Delta < 0$	$j + 2m = \bar{\Delta}$ $0 < \bar{\Delta} < 2/3j$
1. ++ ++	$4\epsilon - \frac{40}{3}j - \frac{8}{3}\Delta$	$4\epsilon - 8j - 8\bar{\Delta}$	13. + +	$4\epsilon - \frac{18}{3}j + \frac{6}{3}\Delta$	$4\epsilon - 10j + 6\bar{\Delta}$
2. ++ ○○ --	$4\epsilon - \frac{28}{3}j + \frac{4}{3}\Delta$	$4\epsilon - 12j + 4\bar{\Delta}$	14. - +○++	$4\epsilon - \frac{18}{3}j + \frac{6}{3}\Delta$	$4\epsilon - 10j + 6\bar{\Delta}$
3. -- ++	$4\epsilon - \frac{28}{3}j + \frac{4}{3}\Delta$	$4\epsilon - 12j + 4\Delta$	15. - +○+	$4\epsilon - \frac{18}{3}j + \frac{6}{3}\Delta$	$4\epsilon - 10j + 6\bar{\Delta}$
4. - - ++	$4\epsilon - \frac{28}{3}j + \frac{4}{3}\Delta$	$4\epsilon - 12j + 4\bar{\Delta}$	16. +○+ -○+ -○- or +○-	$4\epsilon - \frac{12}{3}j + \frac{12}{3}\Delta$	$4\epsilon - 12j + 12\bar{\Delta}$
5. ++ ++	$4\epsilon - \frac{28}{3}j - \frac{8}{3}\Delta$	$4\epsilon - 4j - 8\bar{\Delta}$	17. - +○+	$4\epsilon - \frac{10}{3}j + \frac{10}{3}\Delta$	$4\epsilon - 10j + 10\bar{\Delta}$
6. - ○+ ++	$4\epsilon - \frac{26}{3}j + \frac{2}{3}\Delta$	$4\epsilon - 10j + 2\bar{\Delta}$	18. + - -○+	$4\epsilon - \frac{10}{3}j + \frac{10}{3}\Delta$	$4\epsilon - 10j + 10\bar{\Delta}$
7. -- ○ ++	$4\epsilon - \frac{26}{3}j + \frac{2}{3}\Delta$	$4\epsilon - 10j + 2\bar{\Delta}$	19. - -○+ +	$4\epsilon - \frac{10}{3}j + \frac{10}{3}\Delta$	$4\epsilon - 10j + 10\bar{\Delta}$
8. + ++ -	$4\epsilon - \frac{24}{3}j$	$4\epsilon - 8j$	20. - + +○-	$4\epsilon - \frac{10}{3}j + \frac{10}{3}\Delta$	$4\epsilon - 10j + 10\bar{\Delta}$
9. - + ++	$4\epsilon - \frac{24}{3}j$	$4\epsilon - 8j$	21. - - ○ ++	$4\epsilon - \frac{10}{3}j - \frac{2}{3}\Delta$	$4\epsilon - 2j - 2\bar{\Delta}$
10. + - ++	$4\epsilon - \frac{20}{3}j + \frac{8}{3}\Delta$	$4\epsilon - 12j + 8\bar{\Delta}$	22. - - ○ ++	$4\epsilon - \frac{10}{3}j - \frac{2}{3}\Delta$	$4\epsilon - 2j - 2\bar{\Delta}$
11. - ++ -	$4\epsilon - \frac{20}{3}j + \frac{8}{3}\Delta$	$4\epsilon - 12j + 8\bar{\Delta}$	23. + + ○- or ○- +○+ -○+	$4\epsilon - \frac{8}{3}j + \frac{8}{3}\Delta$	$4\epsilon - 8j + 8\bar{\Delta}$
12. + + - -	$4\epsilon - \frac{20}{3}j + \frac{8}{3}\Delta$	$4\epsilon - 12j + 8\bar{\Delta}$			

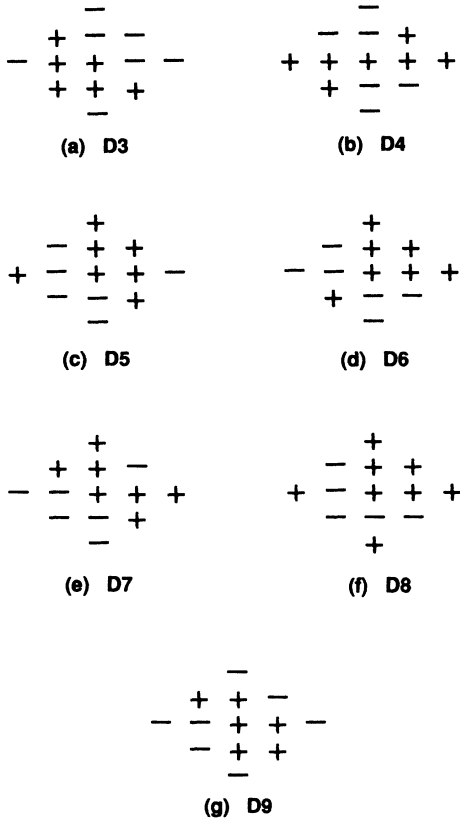


FIG. 4. In (a)–(f) we present the x - y projections of the six optimal one-spin-flip clusters (D3–D8) for the point of degeneracy $P_2(2,0)$. Since all of the zero-temperature states under consideration are translationally invariant in the third spatial direction one need consider only the x - y projections of the spin-flip clusters. In (g) we present the extended cluster (D9) which has a highest one-spin-flip energy, and lowest ground-state site energy.

sions in which translational symmetry exists reduces the number of dimensions in which the problem must be solved. This simplification occurred once before at the degeneracy point R where translational symmetry in two

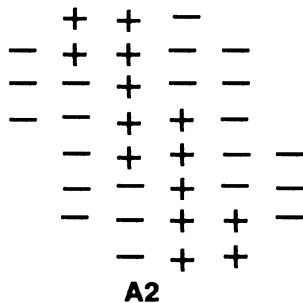


FIG. 5. That phase (A2) which is optimal or equilibrium at the point $P_2(2,0)$. The phase is translationally invariant in the third spatial direction.

directions resulted in essentially a one-dimensional problem.

(b) Any connected four-spin cluster which lies along either the principal x or y directions of the lattice has the same multiplicity since the spin sequences are the same in both phases ($\cdots + + - - + + - - \cdots$).

(c) Any connected four-spin cluster which lies along lattice diagonals in the xy plane has identical multiplicities in both phases. The reason is similar to that for rule (b).

(d) If to a given three-spin-flip cluster we add only linear-next-nearest-neighbor (LNNN) bonds, then the multiplicities of that composite cluster must be the same in both phases. This results from the observation that only unlike LNNN bonds exist on the xy plane.

(e) Any cluster with only LNNN bonds, or at most one nearest-neighbor (NN) or diagonal-neighbor (DN) bond, has the same multiplicity in both phases.

(f) A connected three-spin cluster which lies along an x or y direction and which is terminated with a spin producing a NN and DN bond has the same multiplicity in both phases.

We must now explicitly construct all remaining four-spin clusters which are not rendered irrelevant by these rules. In Table VI we collect these clusters and their excitation energies in terms of the variables j , and Δ of Eq. (3.23).

Now, for small values of Δ it is clear that the dominant fourth-order spin-flip cluster is given in entry 1 in Table VI. One can readily see that the multiplicity of this cluster is different in the two phases. This means that although the leading terms at fourth order in the free-energy density of the two phases will have the same exponential behavior, their coefficients are different. Now, the difference in free-energy densities at Δ is

$$f \langle 2:2:\infty \rangle_D - f \langle 2:2:\infty \rangle \sim -\frac{1}{4}e^{-\epsilon} + \cdots, \quad (3.29)$$

where the ellipsis represents higher-order terms, and

$$\begin{aligned} \epsilon^4 &= 4\epsilon - 13\frac{1}{3}j, \\ \epsilon &= \frac{28}{6}j - \frac{2}{3}\Delta, \end{aligned}$$

and one expects the $\langle 2:2:\infty \rangle$ phase to be favored. We have shown that this result holds for the entire region, rather than just small Δ . The argument is not trivial but follows from careful examination of Table VI. Actually, to our knowledge there exists no rigorous proof that one can resolve between free-energy densities only on the basis of prefactors of exponentially small quantities. In most low-temperature analysis one is able to resolve on the basis of different exponents arising from different spin-flip energies. Since the Pirogov-Sinai theory does not apply at the present degeneracy region we merely assert the sufficiency of (3.29) to establish that the equilibrium phase is $\langle 2:2:\infty \rangle$. It seems very unlikely that this assertion will turn out to be incorrect.

We have now shown that for $\tau > 0$ and $\tau < 0$ the equilibrium phases are, respectively, the $\langle 1 \rangle$ and $\langle 2:2:\infty \rangle$ phases. The situation at $\tau = 0$ is more subtle since here there is an infinite degenerate set of zero-temperature

states. One might expect that, as before, one or more of these phases spring from this zero-temperature-state manifold and there would then be some stable phase inserted between the $\langle 1 \rangle$ and $\langle 2:2:\infty \rangle$ phase. We will soon show this expectation to be incorrect. In fact, at finite temperatures $\langle 1 \rangle$ and $\langle 2:2:\infty \rangle$ phases are found to be equilibrium on a sheet of first-order phase transitions.

The situation is now clear. Along the line $P_2Q_2(\Delta, \tau, T=0)$ the clusters C_2^0 and C_2^1 are energetically degenerate and an infinite number of ground states can be constructed. For $\gamma > 2$, that is, within the strip $P_2Q_2(\Delta, \tau, T=0)$ one has only the $\langle 1 \rangle$ phase. For $\gamma < 2$, that is within the strip $P_2Q_2(\Delta, \tau, T=0)$, the twofold degeneracy is broken in favor of the $\langle 2:2:\infty \rangle$ phase. Our next task must therefore be the examination of the phase structure which, at finite temperature, arises from the line $P_2Q_2(\Delta, \tau=0, T=0)$.

F. Region of degeneracy for $P_2Q_2(\Delta, \tau=0)$

The following arguments are again based on the fact that there is only one single-spin-flip excitation energy in each of the zero-temperature states found along the line $P_2Q_2(\Delta, \tau=0)$. This result can be checked by explicitly constructing all single-spin excitation clusters. We expect the form of the free-energy density up to one-spin-flip order to be

$$f = -\mathcal{N}_2^0 \left[-\frac{7}{6}j + \frac{\Delta}{6} + \frac{1}{3}\tau\Delta - \frac{1}{3}\tau j \right] - (1 - \mathcal{N}_2^0) \left[-\frac{7}{6}j + \frac{\Delta}{6} \right] + e^{-\varepsilon} \left[\sum_{\lambda} a_{\lambda}(\mathcal{N}, \xi) e^{b_{\lambda}(\mathcal{N}_2^0, \xi)} \tau \right],$$

$$\varepsilon = -4 \left[-\frac{7}{6}j + \frac{\Delta}{6} \right], \quad (3.30)$$

$$\mathcal{N}_2^0 = N \frac{(C_2^0)}{L^3},$$

where a_{λ} and b_{λ} are some complicated configuration-dependent functions of $N(C_2^0)$ and other variables ξ . Note that the coefficients a_{λ} satisfy the relation

$$\sum_{\lambda} a_{\lambda} = 1. \quad (3.31)$$

From formula (3.30) we can see that at zero temperature if $N(C_1^0) = 1$, we obtain the ground-state energy per spin of the $\langle 2:2:\infty \rangle$ phase while, if $N(C_2^0) = 0$, we obtain the ground-state energy per spin for the $\langle 1 \rangle$ phase.

We now seek to minimize the free-energy function (3.30) with respect to $N(C_2^0)$ for all $-e^{-\varepsilon} \lesssim \tau \lesssim e^{\varepsilon}(\tau=0)$. Retaining only terms to $O(E^{-\varepsilon})$ we find

$$f = -\mathcal{N}_2^0 \left[-\frac{7}{6}j + \frac{\Delta}{6} + \frac{1}{3}\eta\Delta - \frac{1}{3}\eta j \right] - (1 - \mathcal{N}_2^0) \left[-\frac{7}{6}j + \frac{\Delta}{6} \right] + e^{-\varepsilon}.$$

For $\eta > 0$ this is optimized by the choice $\mathcal{N}_2^0 = 1$ which implies that the $\langle 1 \rangle$ phase is stable. For $\eta < 0$, $\mathcal{N}_2^0 = 0$ and the $\langle 2:2:\infty \rangle$ phase is found to be favored. However, when $\eta = 0$ we find that the zero-temperature states are still degenerate to one-spin-flip order. The two-spin-flip analysis would yield a correction of form

$$\Delta f^{(2)} = e^{-2\varepsilon} (2\mathcal{N}_2^0 + 2\mathcal{N}_2^1) e^{4j} \sum_{\lambda} C_{1\lambda} e^{-\tau d_{1\lambda}} + (3\mathcal{N}_2 + 4\mathcal{N}_2^0) e^{(4/3)(j-\Delta)} \sum_{\lambda} C_{2\lambda} e^{-\tau d_{2\lambda}} + 2\mathcal{N}_2^1 e^{-(2/3)(j-\Delta)} \sum_{\lambda} C_{3\lambda} e^{-\tau d_{3\lambda}} + (\mathcal{N}_2^1 + 3\mathcal{N}_2^0) e^{-(2/3)(j-\Delta)} \sum_{\lambda} C_{4\lambda} e^{-\tau d_{4\lambda}} + (3\mathcal{N}_2^1 + 2\mathcal{N}_2^0) e^{-(4/3)(j-\Delta)} \sum_{\lambda} C_{5\lambda} e^{-\tau d_{5\lambda}} + (\mathcal{N}_2^0 + \mathcal{N}_2^1) e^{-4j} \sum_{\lambda} C_{6\lambda} e^{-\tau d_{6\lambda}} + \sum_{\lambda} f_{\lambda}.$$

At $\tau=0$ the dominant term which has a dependence on the zero-temperature state is

$$\text{const}(3 + \eta_2^0) e^{(4/3)(j-\Delta)}. \quad (3.34)$$

This term is maximized (and hence the free-energy density optimized) when $\mathcal{N}_2^0 = 1$, which implies that the $\langle 1 \rangle$ phase is most stable. When τ is a small positive number of $O(e^{-\varepsilon})$ one again obtains the $\langle 1 \rangle$ phase as the equilibrium phase. When τ is sufficiently negative the $\langle 2:2:\infty \rangle$ phase is stable. We now conclude that no phase besides the $\langle 1 \rangle$ and $\langle 2:2:\infty \rangle$ phases are stable in the vicinity of the line $P_2Q_2(\Delta, \tau=0)$. The $\langle 1 \rangle$ and $\langle 2:2:\infty \rangle$ phases are in equilibrium and at finite temperatures $P_2Q_2(\Delta, \tau, T)$ is a sheet of first-order phase transitions which, near $\Delta=0$, bends in the negative- τ direction.

G. Point of degeneracy P_2 and phase behavior $P_2(\Delta, \tau, T)$ as a function of Δ , τ , and temperature

The reader may recall from earlier descriptions in Sec. III C that we were able to analyze the behavior in the vicinity of the point $P_2(\gamma=2, 0)$ and showed that only three phases, respectively, $\langle 2:2:\infty \rangle$, $A2$, and $\langle 1 \rangle$ are found as γ passes from $\gamma < 2$ to $\gamma > 2$ through the special value $\gamma = 2$. In our earlier discussions we fixed $\Delta = j + 6m = 0$ so we did not consider the possibility that on the plane $\gamma = 2$ other phases might be inserted between the $\langle 1 \rangle$ and $A2$ phases or $A2$ and $\langle 2:2:\infty \rangle$ phase as Δ is varied. In fact, we have examined $P_2(\Delta, \tau = \gamma - 2, T)$ only as a function of Δ or τ for fixed values of τ or Δ , but not in the vicinity where τ is very small and Δ is arbitrary. Actually,

one can make an argument, similar to those of earlier sections, that no phase besides $\langle 1 \rangle$, $\langle 2:2:\infty \rangle$, $\langle 2 \rangle$, and A_2 are stable in this region. In this case we have not been able to make our arguments rigorous.

However, we believe the phase A_2 grows as a conelike protrusion at $\tau=0$ ($\gamma=2$) from the point $P_2(0,0,0)$. In this respect $P_2(0,0,0)$ is a quite remarkable point in the phase diagram. With further effort in our researches it may be possible to prove the uniqueness of the phase A_2 which springs from the degeneracy point $P_2(0,0,0)$.

IV. GENERAL CONCLUSIONS

A low-temperature analysis was carried out to break the degeneracy between periodic and aperiodic states on an infinitely degenerate zero-temperature-state manifold. We were reminded that there may be many degenerate states of a Hamiltonian but that many never appear on the finite-temperature phase diagram. The Hamiltonian itself depended only on short-range forces, but when fluctuations are introduced spins are effectively coupled across longer-length scales. This is the reason that the degeneracy between zero-temperature states breaks as one includes more extended spin-flip excitations. For the low-temperature analysis of aperiodic states it transpires that, since the couplings in the Hamiltonians are fairly local, the information needed to carry out spin-flip calculations is simply local information. Consequently, even if one does not have the simplifying features of regularity and, consequently, structural variables, it is still possible

to make progress. Indeed, one of the lessons one learns from the study of this model is that degeneracy can be completely resolved simply by considering successively larger clusters in the zero-temperature states and deciding which contribute the lowest free-energy density terms. In this way one can, in principle, completely remove the degeneracy and provide a description of the equilibrium low-temperature phase. The basic philosophy underlying the analysis of aperiodic states is a little different from the structural variable analysis of periodic states. In the former case one does not know the symmetry of the state prior to starting the analysis. Actually, tighter constraints are placed on the phase structure at each successive spin-flip order. However, it is sometimes still not possible to explicitly construct the phase without solving a rather difficult packing problem. This packing problem can often be overcome by explicit construction. It is, in any case, a task that is sufficiently well formulated that it may be possible to make general progress in its solution. Complete understanding of certain parts of our phase diagram will probably have to await such progress.

ACKNOWLEDGMENTS

The authors thank Professor B. Widom for many helpful discussions about the problems addressed in this paper. At an early stage of research Professor M. E. Fisher also made many helpful suggestions and we are grateful for this help. Arjun Berera thanks the National Science Foundation for support and Kenneth Dawson gratefully acknowledges the support of the Dreyfus Foundation.

-
- ¹S. A. Pirogov, Ya. G. Sinai, *Theor. Mat. Fiz.* **25**, 358 (1975). V. M. Gerzik, R. L. Dobrushin, *Funkts. Anal. Prilozk.* **8**, 12 (1972); J. Slawny, in *Phase Transitions and Critical Phenomena*, edited by C. Domb and J. L. Lebowitz (Academic, London, 1987), Vol. 11, Chap. 3, and references therein.
- ²S. A. Pirogov and Ya. G. Sinai, *Theor. Mat. Fiz.* **26**, 61 (1976).
- ³For certain selected portions of the phase diagram, for example, in the vicinity of $R(\gamma,0)$, it may be possible to prove such a result. Communication by D. Fisher from Ya. G. Sinai.
- ⁴R. J. Elliot, *Phys. Rev.* **124**, 346 (1961).
- ⁵M. E. Fisher and W. Selke, *Philos. Trans. R. Soc. London* **302**, 1 (1981).
- ⁶R. M. Hornreich, R. Liebmann, H. G. Schuster, and W. Selke, *Z. Phys. B* **35**, 91 (1979); M. N. Barber and W. Selke, *J. Phys. A* **15**, L617 (1982); P. Bak, *Rep. Prog. Phys.* **45**, 587 (1982), and references therein; M. Høgh Jensen and P. Bak, *Phys. Rev. B* **27**, 6853 (1983); W. Selke and P. M. Duxbury, *Z. Phys. B* **57**, 49 (1984); W. Selke, *Phys. Rep.* **170**, 214 (1988), and references therein.
- ⁷K. A. Dawson, B. Walker, and A. Berera (unpublished).
- ⁸K. A. Dawson, M. D. Lipkin, B. Widom, *J. Chem. Phys.* **88**, 5149 (1988).
- ⁹M. D. Lipkin, *Phys. Rev.* **37**, 9512 (1988).
- ¹⁰M. D. Lipkin, *Physica* (to be published).
- ¹¹See AIP document No. PAPS PLRAA-41-626-09 for 9 pages of a table containing all the appropriate information for three-spin-flip excitations at $\gamma=2$. Order by PAPS number

and journal reference from American Institute of Physics, Physics Auxiliary Publication Service, 335 East 45th Street, New York, NY 10017. The prepaid price is \$1.50 for a microfiche or \$5.00 for a photocopy. Airmail additional.

- ¹²The tables which contain all information on the excitations of spins in the layered phases use certain abbreviated notations to describe the excitation cluster. Some of these contractions are probably self-explanatory, for instance, NN, LNNN and DN refer to bonds which are, respectively, nearest neighbors, linear next-nearest-neighbors, and diagonal neighbors. In addition, these bonds between spins may lie either within the same layer (in layer, IL) or in the plane of the paper (in plane IP). Two spins may be separated by one or more boundaries between bands, in which case we refer to them as cross-band (CB) or cross-two-band (C2BS) types. Alternatively, they may lie within a given band when they are referred to as in-band spins (IB).
- ¹³As we pointed out in Sec. II, the zero-temperature states may be determined by writing the energy of an arbitrary spin configuration in terms of the octahedral clusters C_n^N . This energy expression can then be minimized with respect to n and N . Since at least one state can always be composed of a single octahedral cluster and its image under inversion, we can be sure that a global minimum of the energy is located. Certainly this is the most convenient way of breaking up the energy. However, if one examines Eq. (1.1) it is clear that one can also write the energy in terms of clusters of 24 spins consisting of a

central and all connected or coupled spins. We refer to this cluster as an extended or single-spin-flip cluster. We have used this representation of the energy when spin-flip excitation energies are being computed. Thus, to calculate single-spin-flip excitation energies, one needs to know the spin states

of the central and all connected sites. If one is interested in simultaneously minimizing the ground-state and excitation energies then it may be more convenient to base one's calculations on the extended clusters.

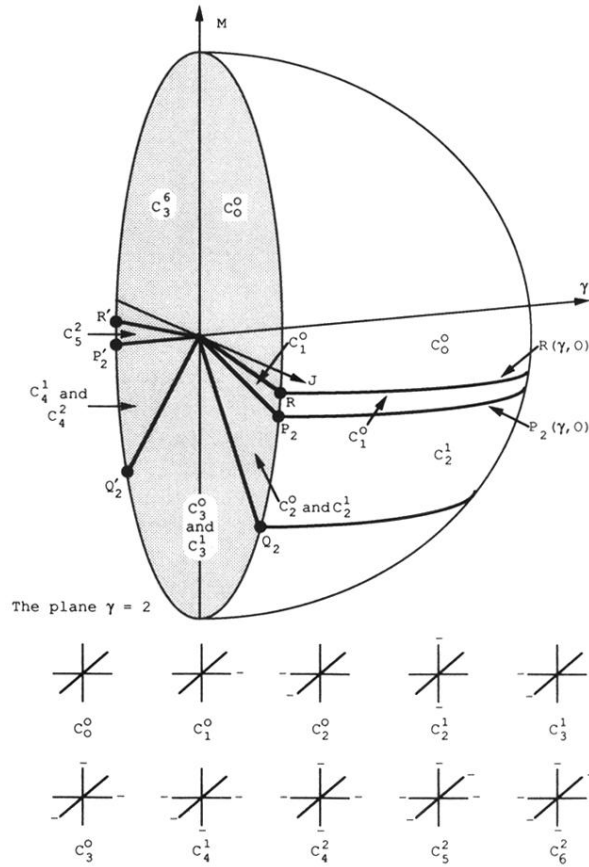


FIG. 1. The zero-temperature phase diagram. In this diagram we illustrate the topology of the zero-temperature-state diagram. Each portion of the diagram is labeled by one or more of the octahedral clusters of spins. These clusters are drawn at the bottom of the figure. Thus, for any choice of J , M and γ one can identify that local cluster, which minimizes the energy density. Typically, along certain surfaces of the zero-temperature-state diagram one has a profound degeneracy in the zero-temperature states. One must resolve this degeneracy using the low-temperature expansion described in the present paper.